Astron. Astrophys. 322, 29–37 (1997)

ASTRONOMY
AND
ASTROPHYSICS

A radio continuum survey of Shapley-Ames galaxies at λ2.8 cm

III. The radio – far infrared correlation

S. Niklas[1,2]

[1] Max-Planck-Institut für Radioastronomie, Auf dem Hügel 69, D-53121 Bonn, Germany
[2] Max-Planck-Institut für Kernphysik, Postfach 10 39 80, D-69269 Heidelberg, Germany

Received 28 May 1996 / Accepted 22 July 1996

Abstract. Radio flux densities of Shapley-Ames galaxies at λ2.8 cm from Niklas et al. (1995a, Paper I) and at λ20 cm from Condon (1987, C87) have been used to investigate the radio – far infrared (FIR) correlation at two different radio wavelengths. The correlation between monochromatic radio and the FIR luminosity was found to be non-linear ($P_{2.8cm} \propto L_{FIR}^{1.09\pm0.04}$ and $P_{20cm} \propto L_{FIR}^{1.23\pm0.05}$). Galaxies with Seyfert activity often exhibit enhanced radio emission compared to the FIR. Interacting and Starburst Galaxies do not show significant deviations from the correlation. For 74 galaxies with separated thermal and non-thermal radio emission the thermal radio luminosity was found to be proportional to the FIR luminosity. At both frequencies the non-thermal radio luminosity is non-linearly connected to the FIR luminosity ($P_{nth} \propto L_{FIR}^{1.25\pm0.08}$). From the ratio P_{th}/L_{FIR} one can conclude that $\simeq$ 30 % of the FIR emission can be attributed to dust associated with massive star-forming regions.

Key words: galaxies: spiral – infrared: galaxies – radio continuum: galaxies – ISM: cosmic rays

1. Introduction

A correlation between the radio and the far infrared emission was first detected by de Jong et al. (1985) for a large sample of spiral galaxies at a wavelength of λ6.3 cm and by Dickey & Salpeter (1984) in galaxies of the Hercules Cluster. The importance of the correlation became more and more obvious in the following years. It holds over four orders of magnitude in luminosity and is valid for all kinds of star forming galaxies e.g. normal Sbc spirals (Hummel et al. 1988), spirals and irregulars (Wunderlich et al. 1987, Wunderlich & Klein 1988), Blue Compact Dwarf Galaxies (Klein et al. 1991), and for cluster galaxies (Helou et al. 1985).

The correlation does not just reflect a 'richness effect' (Xu et al. 1994a), but can be attributed to a coupling between the dust-heating photons, emitted by young, massive stars, and the synchrotron-emitting relativistic electrons of the cosmic rays. Hence, the correlation is valid for the emission of the star-forming disk. This is further supported by the fact that the correlation also holds on kiloparsec scales within galaxies (e.g. Beck & Golla 1988, Bicay et al. 1989, Bicay & Helou 1990, Fitt et al. 1992, Xu et al. 1992).

For galaxies containing an active nucleus the correlation does not hold. Sopp & Alexander (1991) showed that the radio emission of radio galaxies and radio-loud quasars is enhanced by two orders of magnitude compared to normal galaxies.

The tightness of the correlation is astonishing due to the different physical mechanisms producing the radio and FIR emission. In general, the existence of the correlation is explained by attributing the origins of the cosmic ray electrons and the dust-heating photons to the same young star population. A theoretical approach to the correlation was the so-called calorimeter model of Volk (1989). The model assumes that the relativistic electrons are completely trapped in their host galaxies and that the galaxies are optically thick for the dust-heating stellar UV photons. The FIR emission of the galaxies is assumed to be proportional to the supernova rate. The same stellar population is thought to be responsible for the production of cosmic ray electrons. Additionally, a proportionality between the energy densities of the magnetic field and the interstellar radiation field is required. A more general approach by Lisenfeld et al. (1996) allows finite escape probabilities for the cosmic-ray electrons and finite optical depth for the stellar UV radiation as well as an outward gradient in the magnetic field strength. Regarding the synchrotron emission, Pohl (1994) developed a more general approach to this problem, including all kinds of energy losses of the cosmic rays.

Helou & Bicay (1993) argued that the correlation should also hold for optically thin galaxies and high escape probabilities for the electrons. This requires that the efficiency of extracting synchrotron emission from the cosmic ray electrons and the absorption of the dust-heating UV photons are proportional to each other. The coupling between the two mechanisms is produced by a relation between the magnetic field and the density

Send offprint requests to: S.Niklas

of the interstellar gas. Such a relation has been found within galaxies on different spatial resolutions, e.g. in a spiral arm region southwest of the M 31 centre (Berkhuijsen et al. 1993) as well as in the Milky Way (Berkhuijsen, in prep). Also on global galactic scales such a relation is valid (Niklas & Beck 1996). On the other hand the model by Helou & Bicay (1993) predicts a linear correlation between the radio and FIR luminosity. This is clearly not the case (e.g. Table 1 in Price & Duric 1992).

The non-linearity opens another field of discussion. Fitt et al. (1988) assumed that the FIR emission can be decomposed in a 'warm' component related to the formation of massive stars and a 'cold', cirrus component due to low mass stars. Each component is characterized by a colour temperature defined by the ratio of the FIR fluxes at 60 μm and 100 μm. The cold component should not contribute to radio emission. However Xu et al. (1994b) showed that the 'cold' FIR-component correlates even better with the radio than the 'warm' component. In another attempt to explain the non-linearity Chi & Wolfendale (1991) proposed that the increasing escape probability of the cosmic-ray electrons towards less luminous galaxies leads to a faster decrease in synchrotron luminosity than in FIR luminosity. According to their model the slope should become unity in the high luminosity range. But due to the findings of Wielebinski et al. (1987) the slope increases with increasing luminosity. Xu et al. (1994a) showed that the non-linearity of the correlation could be the result of different dependencies of radio and far infrared emission on the star-formation rate, which is even more pronounced if mass-normalized fluxes are considered. Similar arguments had been advanced before by Condon et al. (1991). For a sample of 31 galaxies Price & Duric (1992) showed that the thermal radio emission is directly proportional to the FIR emission and that the non-linearity may be produced by the synchrotron component.

Because of the importance of star formation for the interpretation of the correlation the investigation of the connection between high-frequency radio data and the FIR emission of galaxies is important. The connection of high-frequency radio data with star formation is closer because of the higher fraction of thermal emission. Radio data at such high frequencies are also needed for the separation of thermal and non-thermal radio emission because they do not suffer from optical extinction as Hα emission. For a sample of 74 galaxies thermal and non-thermal radio emission was separated by Niklas et al. (1996, Paper II) based upon the data set presented by Niklas et al. (1995a, PaperI). The large set of λ2.8 cm fluxes from Paper I will be used to establish the radio-FIR correlation at 10.55 GHz and investigate the influence of morphology on the position of a galaxy within the correlation (Section 2). In Section 3 individual galaxies will be discussed and the influence of core emission on the correlation is investigated. The correlation between the thermal radio and the FIR emission and between the non-thermal and FIR luminosity is presented in Section 4. Finally, we discuss the question of cosmic ray confinement in spiral galaxies.

2. The radio-FIR correlation at λλ20 and 2.8 cm

According to Helou et al. (1988) the FIR flux between $\lambda \sim 40\,\mu$m and $\lambda \sim 120\,\mu$m can be estimated using the 60 μm S_{60} and 100 μm S_{100} flux densities from the IRAS data:

$$\left(\frac{\mathrm{FIR}}{\mathrm{W\,m^{-2}}}\right) = 1.26 \times 10^{-14} \left(\frac{2.58\mathrm{S}_{60} + \mathrm{S}_{100}}{\mathrm{Jy}}\right) \quad (1)$$

With the distance of the galaxies and FIR one can compute the FIR luminosity L_{FIR} of the galaxy between $\lambda = 40\,\mu$m and $\lambda = 120\,\mu$m.

For 184 galaxies of the Shapley-Ames survey L_{FIR} and the monochromatic radio luminosities at λ2.8 cm $P_{2.8cm}$ were available (Table 1 and 2 in Paper I). The IRAS FIR fluxes were extracted from Fullmer & Lonsdale (1989). For the same sample the 1.49 GHz-radio luminosities P_{20cm} were obtained from Condon (1987). In Fig. 1 the radio luminosities at $\lambda\lambda$2.8 and 20 cm were plotted against L_{FIR}. A normalisation of the luminosities on the optical surface of the galaxies does not significantly change the slope of the correlation. An increase in scatter at the low-surface brightness end of the normalised correlation can be due to observational uncertainties. However, it can also be produced by a radio-quiet FIR component as proposed by Xu et al. (1994a). At 10.55 GHz the errors in $P_{2.8cm}$ were calculated using the errors given in the flux densities at λ2.8 cm (Paper I) and gaussian error propagation. The errors in the radio flux densities at 1.49 GHz from Condon (1987) correspond to the uncertainty due to confusion with background sources σ_c. According to Condon (1987) σ_c can be approximated by $\sigma_c \sim \sqrt{270\Omega_b S}$ where Ω_b is the effective solid angle of a Gaussian beam and S the total flux density of the source. For both radio frequencies the radio luminosity is correlated well with the FIR luminosity. A linear fit to the data, using the Bisector-Method by Isobe et al (1990) yields the following results:

$$\log(\mathrm{P}_{2.8cm}) = (-18.55 \pm 1.37) + (1.09 \pm 0.04) \times \log(\mathrm{L}_{FIR}) \quad (2)$$

and

$$\log(\mathrm{P}_{20cm}) = (-23.33 \pm 1.82) + (1.23 \pm 0.05) \times \log(\mathrm{L}_{FIR}) \quad (3)$$

The fit results are represented by the solid lines in Fig. 1. At 10.55 GHz the scatter in the correlation is somewhat larger. This may be due to the smaller flux densities at the higher frequency which leads to higher observational errors. The correlation coefficients of the correlations are $cc_{2.8cm} = 0.92$ and $cc_{20cm} = 0.94$, respectively. There is a significant difference in slope between 1.49 and 10.55 GHz. The slope of the λ2.8 cm correlation is flatter and nearer to unity. This can be produced by the higher amount of thermal emission at λ2.8 cm or by a flatter correlation between the synchrotron emission and the FIR. This question will be discussed in Section 4.

Fig. 2 presents the radio-FIR correlation at λ2.8 cm subdivided into subsamples containing the different morphological types of the galaxies ranging from early spiral galaxies (top, left) to irregular and amorphous galaxies (bottom, right). One can clearly see, that the tightness of the correlation is produced

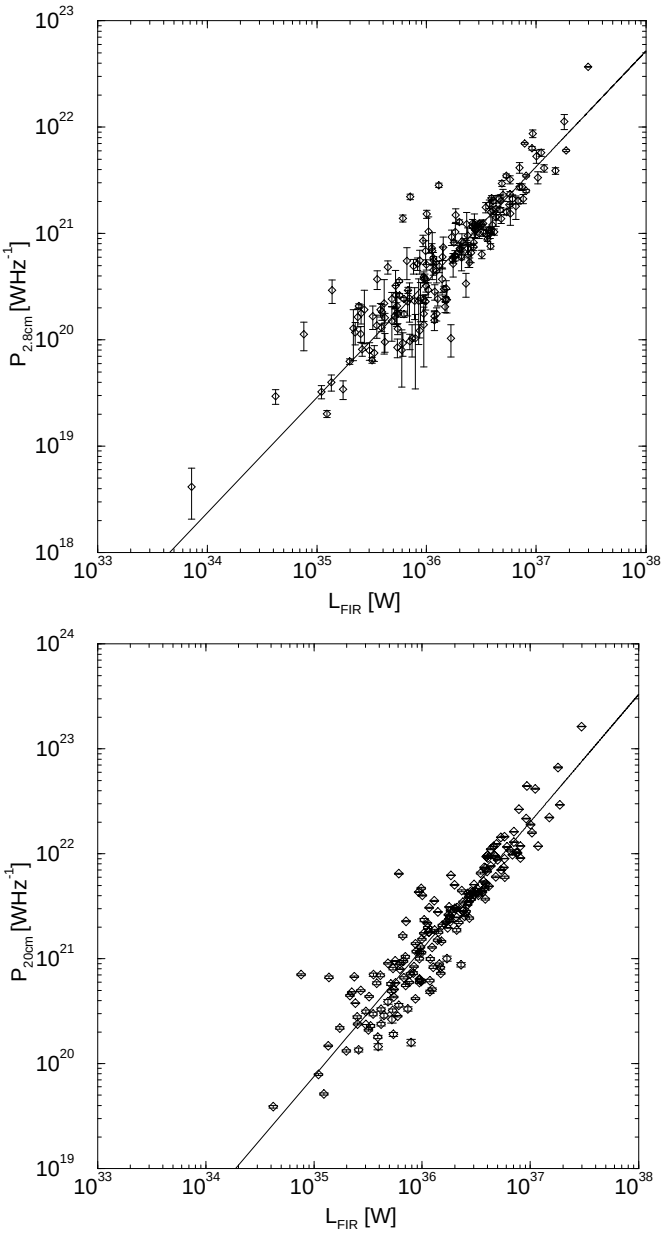

Fig. 1. The radio-FIR correlation at two different radio frequencies. The upper diagram shows the monochromatic radio luminosity at 10.55 GHz plotted versus the FIR luminosity, and the lower one the λ20 cm luminosity versus L_{FIR}

by the emission of galaxies of type Sb and later. The early type Sa/Sab galaxies where the emission of the core is more prominent (Paper I) exhibit a much larger scatter. The correlation coefficients of the subsamples are:
$cc_{Sa/Sab}$ = 0.50 (24 galaxies)
$cc_{Sb/Sbc}$ = 0.90 (74 galaxies)
$cc_{Sc/later}$ = 0.94 (78 galaxies)
$cc_{Irr/Am}$ = 0.93 (8 galaxies)
It is remarkable that the irregular and amorphous galaxies, even though some of them showing strong interactions and disturbances in their interstellar medium show a very strong correlation. For the λ20 cm correlation the result of the subdivision in different galaxy types is similar.

This result supports the view that the radio-FIR correlation is produced by the radio emission of the star forming disk as proposed by various models (Völk 1989, Helou & Bicay 1993, Lisenfeld et al. 1996). The influence of core emission seems to produce a deviation from the correlation. This is discussed in more detail in the following sections.

In order to quantify the position of a galaxy within the correlation the quantity r_λ will be introduced. It is defined in the following way:

$$r_\lambda = \log\left(\frac{P_\lambda}{10^{a_\lambda + s_\lambda \times \log(L_{FIR})}}\right) \quad (4)$$

a_λ and s_λ are intercept and slope of the correlations at the corresponding wavelengths as given in Eqs. 2 and 3. Therefore r_λ defines the ratio between the observed radio luminosity at wavelength λ and the expected radio luminosity concerning L_{FIR}. The distributions of $r_{2.8cm}$ and r_{20cm} peak at zero and have standard deviations of 0.25 and 0.23, respectively. Fig. 3 shows the plot of $r_{2.8cm}$ versus r_{20cm}. The data points are not randomly distributed. There exists a clear correlation between $r_{2.8cm}$ and r_{20cm}. This means that the variations in r_λ are not only due to observational scatter. This is especially true for galaxies with $|r_\lambda| > 0.5$ where the deviation from the correlation is more than 2σ. For galaxies with $|r_\lambda| \lesssim 0.25$ the deviation is in the range of 1σ and therefore not significant. For galaxies with $0.25 \lesssim r_\lambda \lesssim 0.5$ a decision on the significance of a real deviation from the correlation can not be given straightforward. It has to be discussed individually.

3. Discussion of the global radio-FIR correlation

3.1. Individual galaxies

Table 1 shows some representative galaxies with extreme values in r_λ, but also some galaxies with $|r_\lambda| < 0.3$ and pecularities in their other properties. Cols. 1 and 2 give name and morphological types of the galaxies. The latter quantity was extracted from the RSA. The next two columns present the values of r_{20cm} and $r_{2.8cm}$. Some short comments on the individual properties of the galaxies are listed in the last column. More detailed information about these galaxies can be found in Paper I.

The strongest radio emission compared to the FIR is exhibited by galaxies with Seyfert nuclei (e.g. NGC 4594). The radio observations of two galaxies (NGC 4236 and NGC 4656) are strongly disturbed by background sources. Therefore the large values of r_λ seem to be artificial. Some galaxies of the Virgo cluster also show a radio excess. As discussed by Niklas et al. (1995b) galaxies in the inner part of the cluster tend to exhibit a radio excess. Additionally, these galaxies also show signs of nuclear activity. The amount of atomic hydrogen in these galaxies is very low compared with field galaxies (Cayatte et al. 1990). This may be an effect of ram pressure stripping by the Intra Cluster Medium. But there also exist galaxies in the Virgo Cluster with no significant deviation from the radio-FIR correlation (e.g. NGC 4501, NGC 4321). These galaxies are located in the

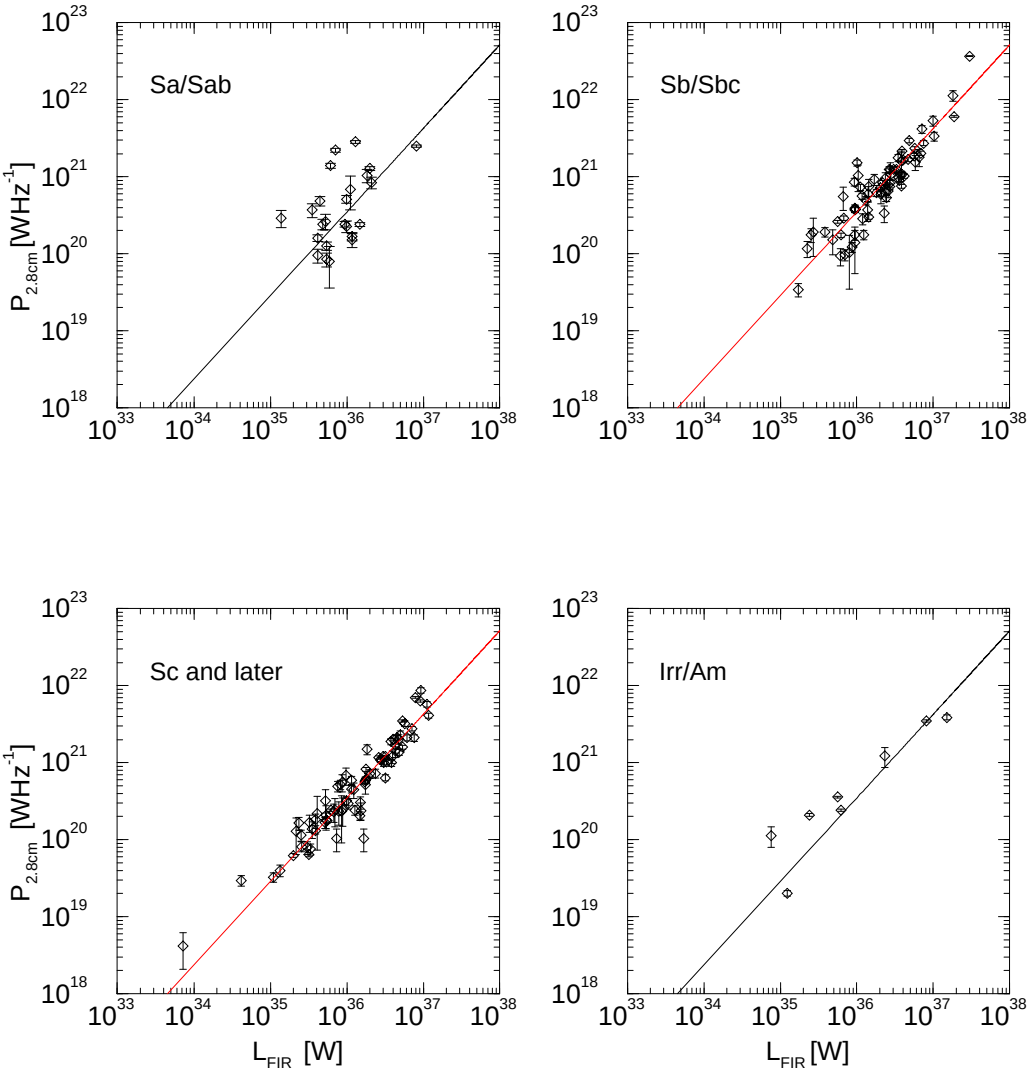

Fig. 2. The radio-FIR correlation at 10.55 GHz subdivided into the different morphological types. The solid lines represent the best fit to the whole sample according to Eq. 2

outer part of the Cluster and their ISM seems not to be affected so strongly by the cluster environment. Nevertheless, it remains unclear if the deviation of Virgo galaxies from the correlation is only due their nuclear actvitiy. The accumulation of deviating, early-type galaxies in the centre of the cluster may be attributed to the morphology-density relation (Dressler 1980). But a real enhancement of the disk radio emission and/or an attenuation of the FIR emission cannot be excluded. This question will be adressed by observations of Virgo Galaxies using the ISO observatory.

Some galaxies seems to have a radio deficit at at least one frequency. But for these sources the errors in the flux densities are very large. They can be easily indentified in the graphs of Fig. 1 by their large errors in P_λ. A galaxy with a radio deficit which seems to be real is NGC 4699. With the existing radio data the reason for this radio deficit cannot be given.

NGC 253 can be considered as the prototype of a starburst galaxy. At 10.55 GHz it follows the correlation. The radio deficit at λ20 cm may be due to very extended disk emission which has not been detected. Therefore a deviation from the correlation of this galaxy cannot be confirmed. The same is valid by NGC 3034. This famous starburst galaxy lies almost perfect on the radio-FIR correlation at both frequencies. It seems that the starburst increases radio and FIR emission at constant proportions and on nearly the same time scales.

Some prominent examples for interacting galaxies are NGC 4038/39 (The Antennae) and NGC 2276. Both galaxies do not show significant deviations from the correlation.

The analysis of some representative galaxies of the sample showed that deviations from the correlation are generally produced by the emission of an active nucleus. Interacting or Starburst galaxies show strong radio and FIR emisssion. But they cannot be distinguished from normal star-forming galax-

Table 1. Positions of some representative galaxies in the radio-FIR correlation

Galaxy	Type	r_{20cm}	$r_{s.8cm}$	Comments
NGC 253	Sc[s]	-0.33±0.03	-0.12±0.03	starburst galaxy
NGC 1068	Sb[rs]II	0.32±0.03	0.40±0.01	core-dominated radio emission, Seyfert nucleus
NGC 2276	Sc[r]II-III	0.25±0.03	0.06±0.01	interacting galaxy
NGC 2655	Sa pec	0.98±0.09	0.81±0.02	Seyfert galaxy
NGC 3034	Am	-0.13±0.01	-0.01±0.01	starburst galaxy
NGC 3079	Sc pec	0.23±0.002	0.31±0.02	nuclear actvity
NGC 3718	Sa pec	0.79±0.08	0.86±0.01	nuclear activity, interaction with near neighbour
NGC 3953	SBbs[r]I-II	-0.00±0.01	-0.37±0.27	extremely large errors in radio fluxes
NGC 4038	Sc pec	0.06±0.01	0.19±0.01	The 'Antennae'
NGC 4236	SBdIV	0.81±0.08	0.55±0.01	possibly confused by background source
NGC 4321	SC[s]I	0.17±0.02	0.04±0.01	Virgo Cluster
NGC 4438	Sb (tides)	0.51±0.05	0.61±0.01	Virgo Cluster, strongly influenced by Intra Cluster Medium
NGC 4450	Sab pec	-0.21±0.02	0.50±0.02	Virgo Cluster
NGC 4501	Sbc[s]II	0.15±0.02	0.00±0.02	Virgo Cluster
NGC 4535	SBc[s]I	-0.02±0.01	-0.77±0.40	large error in flux density at 10.55 GHz
NGC 4579	Sab[s]II	0.32±0.03	0.76±0.03	Virgo Cluster, LINER
NGC 4594	Sa+/Sb-	0.45±0.05	0.96±0.02	Seyfery galaxy
NGC 4656	Am	1.12±0.11	0.72±0.01	confused by background sources
NGC 4689	Sc[s]II	-0.41±0.12	-0.38±0.14	large uncertainty in radio fluxes
NGC 4699	Sab[rs]	-0.45±0.05	-0.39±0.09	no pecularities

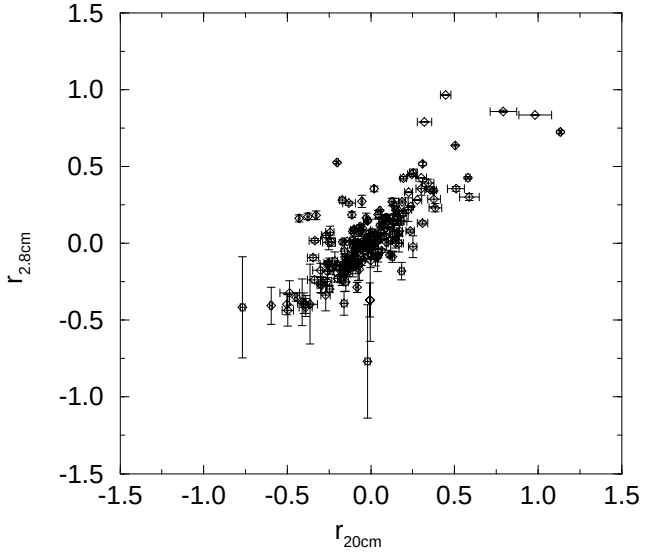

Fig. 3. The ratio between observed and expected radio luminosity at 1.49 and 10.55 Ghz plotted versus each other. The errors in r_λ take into account the errors in radio flux and the errors in the fit

ies on the basis of their position in the radio-FIR correlation. This confirms the view that the correlation is produced by emission where the underlying process is star formation. Hence, the position of a galaxy in the radio-FIR correlation may be used to decide if the radio emission is produced mainly by star formation or by a single central engine even if the spatial resolution of the radio measurement does not allow a separation of disk and core emission.

3.2. Correction of the correlation

It was shown that the influence of nuclear activity can strongly affect the position of a galaxy in the radio-FIR correlation. Hence, a subtraction of the amount of core emission from the total emission should improve the correlation.

For such a correction all galaxies of the sample, which are classified as Seyfert I, Seyfert II or LINER according to Véron-Cetty & Véron (1993), were selected. Furthermore NGC 3079 which shows clear signs of nuclear activity (e.g. Filippenko & Sargent 1992) was included. The amount of radio emission from the nuclei of these 23 galaxies the peak flux densities S_{Peak} given in Table 2 of Paper I was used. It was subtracted from the integrated flux density S_{tot}. Then the corrected monochromatic radio luminosity was calculated. For the same galaxies the correction at 1.49 GHz was carried out using the peak flux densities given in Table 2 of C87. A Bisector-Fit to the data yields the same results as Eqs. 2 and 3 within the errors. Hence, the influence of Seyfert galaxies can not explain the non-linearity of the correlation. Additionally it shows that the total radio emision of the majority of the Shapley-Ames galaxies is dominated by the diffuse disk emission.

For the corrected correlation r_λ was recalculated. The standard deviations of $r^{cor}_{2.8cm}$ and r^{cor}_{20cm} are 0.21 and 0.24, respectively. This shows a slight improvement of the correlation after the subtraction of the nuclear component.

Some galaxies, which have positive r_λ before the subtraction of the core flux, now have negative values. This may come from an overestimate of the core fluxes, which is a consequence of a lack of spatial resolution. At both frequencies the resolution is in the range of 70″. For a galaxy at a distance of 20 Mpc this cor-

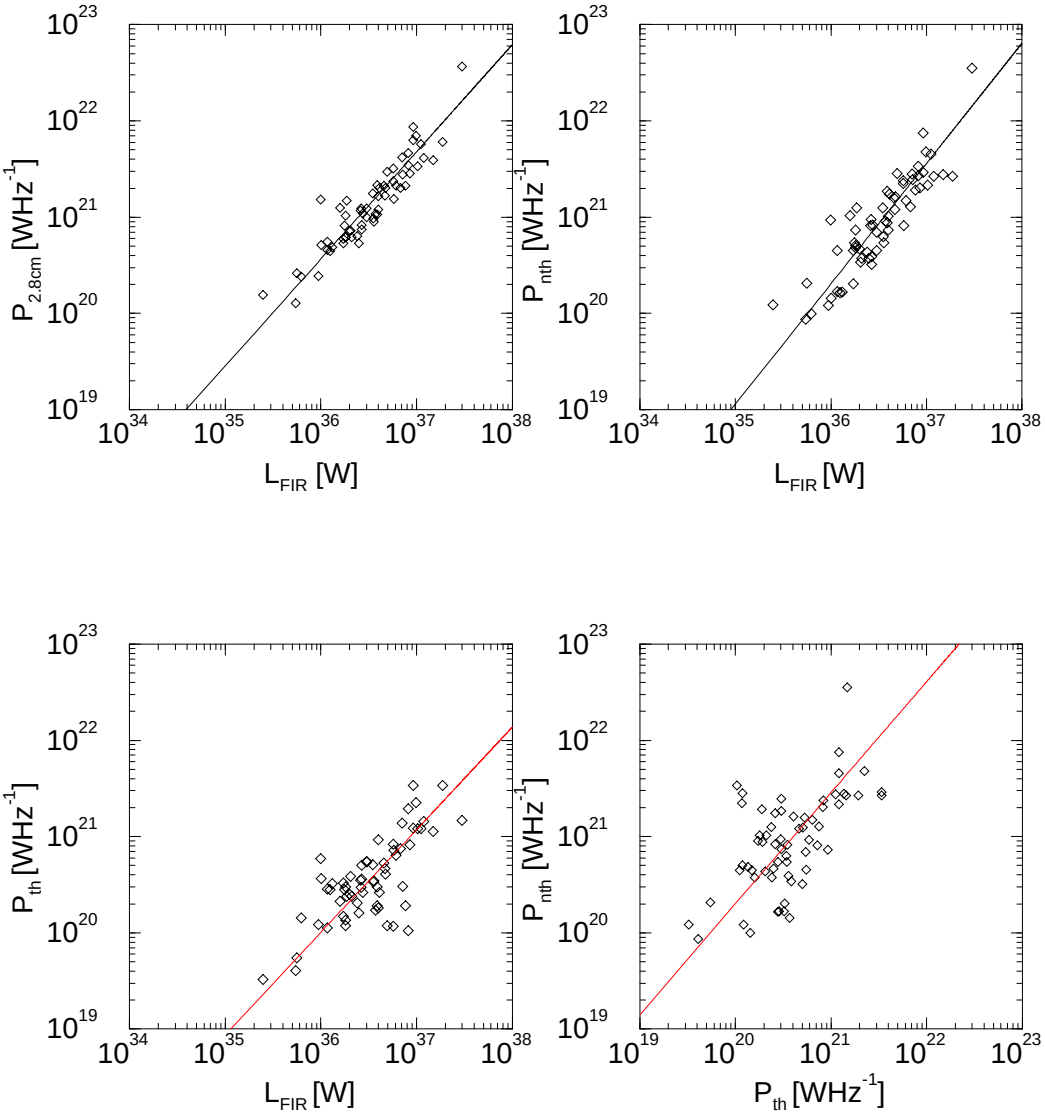

Fig. 4. The radio-FIR correlation at λ2.8 cm for 74 galaxies with separated thermal and non-thermal radio emission. The upper row shows the plot of $P_{2.8cm}$ versus L_{FIR} (left) and of P_{nth} versus L_{FIR} (right). The graphs in the bottom row shows P_{th} versus L_{FIR} and P_{nth} versus P_{th}. The solid lines represents the Bisector-Fit results (Eq. 5 for P_{nth} versus L_{FIR} and Eq. 6 for P_{th} versus L_{FIR})

responds to ∼ 7 kpc. Therefore the corrected radio luminosities are too small.

The fact that some galaxies with Seyfert activity do not strongly deviate from the correlation, but that others hold extreme positions in the radio-FIR correlation may be a consequence of different ratios between core and disk emission. This is supported by the fact that mainly Seyfert galaxies of type Sa and Sab exhibit significant deviations. In comparison, Seyfert galaxies of late type (e.g NGC 5033, NGC 5194), where disk emission is more prominent, scarcely deviate from the radio-FIR correlation.

4. Thermal and non-thermal radio emission

The radio continuum emission of galaxies consists of a thermal component and the synchrotron component. The thermal free-free emission of electrons in HII regions around young, massive stars should be closely connected to the FIR emission. For the synchrotron component one has to take into account the diffusive and convective transport of the cosmic rays, as well as the properties of the interstellar magnetic field. Hence, the coupling between the synchrotron and FIR emission is less obvious.

For 74 galaxies thermal and non-thermal radio emission has been separated by Niklas et al. (1996). For each of these galaxies the thermal fraction f_{th}^{1GHz} at 1 GHz and the non-thermal spectral index α_{nth} were derived, assuming optically thin thermal radio emission and a power-law nature of the synchrotron emission. The thermal fraction f_{th}^{10GHz} at 10 GHz is also given. Using f_{th}^{1GHz} and f_{th}^{10GHz} the thermal flux density S_{th} was evaluated using the total flux density S_{tot} at the corresponding wavelengths. The non-thermal flux density was then computed in the following way $S_{nth} = S_{tot} - S_{th}$. This allows to determine the thermal P_{th}

and nonthermal radio luminosities P_{nth} at 1.49 and 10.55 GHz for the 74 galaxies with separated thermal and non-thermal radio emission.

P_{th}, P_{nth} and the monochromatic, total radio luminosity $P_{2.8cm}$ at 10.55 GHz of these 74 galaxies were plotted versus L_{FIR} (Fig. 4). The Bisector-Fit to the total radio versus FIR luminosity gives no difference to the result for the whole sample (Eqs. 2 and 3). Hence, the subsample of the 74 galaxies follow the same radio-FIR correlation as the complete Shapley-Ames sample (Fig. 4, top, left). A linear Bisector-Fit was done to P_{th} and P_{nth} versus L_{FIR} at $\lambda\lambda 20$ and 2.8 cm. The results at $\lambda 2.8$ cm are:

$$\log(P_{nth}) = (-24.74 \pm 3.26) + (1.25 \pm 0.09) \times \log(L_{FIR}) \quad (5)$$

$$\log(P_{th}) = (-18.33 \pm 2.46) + (1.06 \pm 0.07) \times \log(L_{FIR}) \quad (6)$$

The correlation coefficients are 0.91 for the $P_{nth} - L_{FIR}$ and 0.81 for the $P_{th} - L_{FIR}$ correlation. Fig. 4 and the fit results show that clear correlations exist between thermal and FIR luminosity and between the synchrotron component and the FIR. The slope of the thermal radio-FIR correlation is equal to unity within the uncertainty. The non-thermal correlation shows the same slope at both frequencies within the errors and the slope is significant different from 1. Hence, the non-linearity of the correlation is the result of the non-linear relation between the synchrotron emission and L_{FIR}. The steep synchrotron spectrum produces a ratio between P_{nth} at 1.49 GHz and 10.55 GHz of $\sim 5 - 10$. The slope > 1 of the $P_{nth} - L_{FIR}$ correlation also yields the non-linear dependence (slope = 1.15) between the synchrotron and the thermal radio luminosity.

This result confirms the work by Price & Duric (1992). They found a linear relationship between the thermal radio and FIR luminosity. The correlation coefficient they found is somewhat higher than in this work. But their sample consists only of 31 galaxies. Hence, the significance of the results presented here is higher. For the non-thermal radio correlation Price & Duric (1992) found a slope of 1.33 ± 0.10. This is in good agreement with the result given in Eq. 5. Price & Duric (1992) also discussed the possibility that the thermal and non-thermal radio-FIR correlation is produced by a random process. They found that their component relations have only a very small probability by being generated by a random separation process. This is also valid for this work, because of the higher number of galaxies, which increases the statistical significance and because of the careful separation of thermal and non-thermal radio emission using the radio spectra and Hα data for testing.

From these results one can conclude that the different slopes in Eqs. 2 and 3 are due to the different amount of thermal radio emission at the different frequencies. The higher fraction of thermal emission and the linear dependance of the thermal radio emission from the FIR emission causes the flatter slope of the $\lambda 2.8$ cm correlation. In general the slope of the correlation should decrease with increasing frequency due to the growing amount of thermal radio emission.

The thermal radio luminosity can be used for an estimate of the amount of FIR emission which is emitted by dust heated by massive stars ($> 20 M_\odot$) in star-forming regions. This amount of FIR emssion is the so-called warm FIR-component L^w_{FIR} (Xu et al. 1994b). The ratio between L^w_{FIR} and the Hα-luminosity can be expressed by the mean 'infrared excess' (IRE) of a galaxy. The IRE is defined as (Mezger 1978):

$$\mathrm{IRE} = \frac{L^w_{FIR}}{N^{ion}_e h\nu_{Ly\alpha}} \quad (7)$$

where L^w_{FIR} is the total FIR luminosity of the HII region, N^{ion}_e the number of Lyman continuum photons needed for gas ionisation and $h\nu_{Ly\alpha}$ the energy of a Lyman α photon. This is valid for a single HII region, but in this case it is used for individual galaxies containing many such HII regions. The mean IRE for galaxies is according to Xu et al. (1994b) IRE = 5.3 ± 1.0 yielding to $L^w_{FIR} = 37.5 \times L_{H\alpha}$. According to HII region models (e.g. Caplan & Deharveng 1986) the Hα flux density can be evaluated using the thermal radio flux:

$$S_{H\alpha} = 8 \times 10^{-10} \left(\frac{T}{10^4 K}\right)^{-0.59} \left(\frac{\nu}{10^9}\right)^{-0.1} \times S^\nu_{th} \quad (8)$$

where S^ν_{th} is in Jy and $S_{H\alpha}$ in erg cm^{-2}s^{-1}. Hence, $L_{H\alpha}$ can be expressed by the thermal radio luminosity. With the number of IRE adopted by Xu et al. (1994b) the ratio between the thermal radio luminosity and the warm FIR-luminosity is $L^w_{FIR}/P^{1GHz}_{th} = 2.75 \times 10^{15}$ at 1 GHz and $L^w_{FIR}/P^{10GHz}_{th} = 2.18 \times 10^{15}$ at $\lambda 2.8$ cm. The total FIR luminosity L_{FIR} is the sum of L^w_{FIR} and L^c_{FIR}, which is emitted by dust heated by the interstellar radiation field. Introducing the ratio $R_w = L^w_{FIR}/L_{FIR}$ and using the above derived relations R_w is given by:

$$R_w = 2.75/2.18 \times 10^{15} \left(\frac{P^{1/10GHz}_{th}}{L_{FIR}}\right) \quad (9)$$

For the galaxies with separated thermal and non-thermal emission the ratio $P^{1/10GHz}_{th}/L_{FIR}$ is known and therefore R_w can be computed. The derived mean values for the distribution of R_w are $\langle R_w \rangle = 0.35$ and $\langle R_w \rangle = 0.30$ compiled at 1 and 10 GHz, respectively. The standard deviation of both distributions is $\simeq 0.2$. This means that dust heating by the interstellar radiation field is for most of the galaxies the dominant process. This is in agreement to the findings of Xu et al. (1994b).

5. Particle confinement

The question how efficient the cosmic ray particles are confined in their host galaxies is of great importance for the understanding of the radio-FIR correlation. The asymptotic calorimeter model of Völk (1989) assumes an efficient particle confinement and therefore expects a synchrotron spectral index of the galaxies of ~ 1. Indeed, galaxies with non-thermal spectra of $\alpha_{nth} \simeq 1$ exhibit other indications of being optically thick for cosmic rays and they follow the radio-FIR correlation (Niklas & Beck 1996). However, a significant number of the 74 galaxies with separated thermal and non-thermal radio emission have flatter synchrotron

spectra and do not show significant deviations from the radio-FIR correlation. Convection as a possibly important contributor to electron transport implies flatter spectra at intermediate frequencies. Additionally, Irregular and Blue Compact Dwarf Galaxies seem to follow the correlation but they are known to have high, presumably convective escape probabilities for cosmic ray electrons (Klein et al. 1991).

The model of Helou & Bicay (1993) requires the efficiency of extracting synchrotron radiation from the cosmic rays to be proportional to the absorption of the dust heating UV photons. They expect the FIR-luminous galaxies to be more efficient in particle trapping, therefore having steep non-thermal spectra. The less luminous galaxies are expected to have flat synchrotron spectra. But $\alpha_{\rm nth}$ neither correlates with the density of the interstellar radiation field nor with the strength of the interstellar magnetic field (Niklas & Beck 1996).

The non-linearity of the correlation is another problem of existing models. The above results show clearly that $P_{\rm nth} \propto L_{\rm FIR}^{1.25}$. According to Chi & Wolfendale (1990) the non-linearity is the result of a lack of synchrotron emission compared to the FIR. This lack is produced by the high escape probabiltity of the cosmic ray electrons in galaxies with low FIR luminosity. In the high luminosity range the particle confinement becomes more efficient and the slope of the correlation should become unity. In order to test this hypothesis the original galaxy sample was divided into different subsamples. The original sample was used because the dynamic range in $L_{\rm FIR}$ of the 74 galaxies with separated thermal and non-thermal emission is very small. In each subsample galaxies below a certain limit in $L_{\rm FIR}$ were excluded. Then the slopes of the correlation in every subsample were determined. The lower limits were set from $L_{\rm FIR} = 10^{35}$ W (subsample of 181 galaxies) up to $L_{\rm FIR} = 10^{37}$ W (subsample of 6 galaxies) in steps of 0.25 in $\log(L_{\rm FIR})$. Fig. 5 show the derived slopes plotted versus the lower limit of the corresponding subsample at λ2.8 cm. One can clearly see that the slope becomes steeper with increasing luminosity. This is not a selection effect by the deviation of Seyfert galaxies which are more luminous in all bands, as one can see in the graphs where the active galaxies were excluded. The small number of galaxies in the subsample, where the lower limit is $\simeq 10^{37}$ W, causes larger errors in the derived slope. But nevertheless, a flattening of the correlation can be ruled out. This is in accordance with the results of Wielebinski et al. (1987) who also found an increasing slope with increasing luminosity.

To explain these results there are two possibilities: first, the thermal *fraction* of radio emission decreases with increasing FIR-luminosity and therefore the slope of the non-thermal correlation becomes more and more dominant or, second, the $P_{\rm nth} - L_{\rm FIR}$ correlation itself produces the increase in slope. From the results of Niklas et al. (1996) a coupling between thermal fraction and star formation rate, which is nearly proportional to $L_{\rm FIR}$ (e.g. Buat 1992) can be ruled out. With the thermal amount of radio emission being independent of FIR luminosity the variation in slope has to be an intrinsic property of the connection between $P_{\rm nth}$ and $L_{\rm FIR}$. From the observed increase in slope one can conclude that the non-linearity of the $P_{\rm nth} - L_{\rm FIR}$ correlation is not produced by a variation in efficiency of particle confinement.

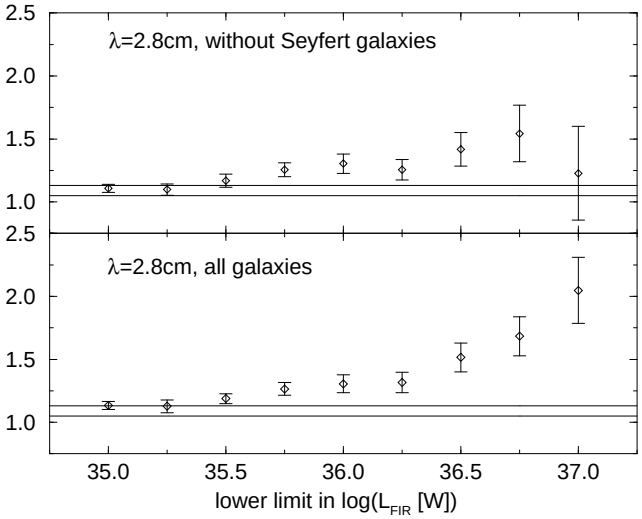

Fig. 5. Analysis of the variation of slope with luminosity at λ2.8 cm. The slopes of the different subsamples were plotted versus the corresponding lower limit in $L_{\rm FIR}$. The lower plot shows the variation in slope for the complete sample, the upper diagram presents the change in slope for a sample of galaxies where all Seyfert galaxies are excluded. The horizontal lines correspond to the range in slope of the complete sample

Acknowledgements. The author wants to thank Profs. R. Wielebinski and U. Klein for their support and help during his PhD. SN is grateful to Prof. H.J. Völk, Dr. R. Tuffs and Dr. C. Xu for stimulating discussions and careful reading of the manuscript.

References

Beck, R., Golla, G. 1988, A&A 191, L9
Berkhuijsen, E.M., Bajaja, E., Beck, R. 1993, A&A 279, 359
Bicay, M.D., Helou, G. 1990, ApJ 362, 59
Bicay, M.D., Helou, G., Condon, J.J. 1989, ApJ 338, L53
Buat, V. 1992, A&A 264, 444
Caplan, J., Deharveng, L. 1986, A&A 155, 297
Cayatte, V., van Gorkom, J.H., Balkowski, C., Kotanyi, C. 1980, AJ 100, 604
Chi, X., Wolfendale, A.W. 1990, MNRAS 245, 101
Condon, J.J. 1987, ApJS 65, 485
Condon, J.J., Anderson, M.L., Helou, G. 1991, ApJ 376, 95
de Jong, T., Klein, U., Wielebinski, R., Wunderlich, E. 1985, A&A 147, L6
Dickey, J.M., Salpeter, E.E. 1984, ApJ 284, 461
Dressler, A. 1980, ApJ 236, 351
Filippenko, A.V., Sargent, W.I.W. 1992, AJ 103, 28
Fitt, A.J., Alexander, P., Cox, M.J. 1988, MNRAS 233, 907
Fitt, A.J., Howarth, N.A., Alexander, P., Lasenby, A.N. 1992, MNRAS 255, 1
Fullmer, L., Lonsdale , C.J. 1989, Catalogued Galaxies & Quasars Observed in the IRAS survey, Version 2, Pasadena: Jet Propulsion Laboratory
Helou, G., Bicay, M.D. 1993, ApJ 415, 93
Helou, G., Soifer, B.T., Rowan-Robinson, M. 1985, ApJ 298, L7

Helou, G. Khan, I.R., Malek, L., Boehmer, L. 1988, ApJS 68, 141
Hummel, E., Davies, R.D., Wolstencroft, R.D., van der Hulst, J.M., Pedlar, A. 1988, A&A 199, 91
Isobe, T., Feigelson, E.I., Akritas, M.G., Babu, G.J. 1990, ApJ 364, 104
Klein, U., Weiland, H., Brinks, E. 1991, A&A 246, 323
Lisenfeld, U., Völk, H.J., Xu, C. 1996, A&A 306, 677
Mezger, P. 1978, A&A 70, 565
Niklas, S., Beck, R. 1996, A&A, in press
Niklas, S., Klein, U., Braine, J., Wielebinski, R. 1995a, A&AS 114, 21
Niklas, S., Klein, U., Wielebinski, R. 1995b, A&A 293, 56
Niklas, S., Klein, U., Wielebinski, R. 1996, A&A, in press
Pohl, M. 1994, A&A 287, 453
Price, R., Duric, N. 1992, ApJ 401, 81
Sopp, H.M., Alexander, P. 1991, MNRAS 251, 14p
Véron-Cetty, M.P., Véron, P. 1993, A Catalogue of Quasars and Active Nuclei (6th Edition), ESO Scientific Report 13
Völk, H.J. 1989, A&A 218, 67
Wielebinski, R., Wunderlich, E. Klein, U., Hummel, E. 1987, in Star Formation in Galaxies, ed C.J. Lonsdale Persson (NASA CP2466), p589
Wunderlich, E., Klein, U., 1988 A&A 206, 47
Wunderlich, E., Klein, U., Wielebinski, R. 1987, A&AS 69, 487
Xu, C., Klein, U., Meinert, D., Wielebinski, R., Haynes, R.F. 1992, A&A 257, 47
Xu, C., Lisenfeld, U., Völk, H.J., Wunderlich, E. 1994a, A&A 282, 19
Xu, C., Lisenfeld, U., Völk, H.J. 1994b, A&A 285, 19

This article was processed by the author using Springer-Verlag LaTeX A&A style file *L-AA* version 3.